Paper-based microfluidic devices by asymmetric calendaring

S. Oyola-Reynoso,[1] C. Frankiewicz,[1] B. Chang,[1] J. Chen,[1] J.-F. Bloch,[2] and M. M. Thuo[1]
[1]*Department of Materials Science and Engineering, Iowa State University, 528 Bissel Rd, Ames, Iowa 50011, USA*
[2]*Department of Paper and Biomaterials, Grenoble Institute of Technology, 38041 Grenoble Cedex 9, France*

(Received 2 November 2016; accepted 2 January 2017; published online 10 January 2017)

We report a simple, efficient, one-step, affordable method to produce open-channel paper-based microfluidic channels. One surface of a sheet of paper is selectively calendared, with concomitant hydrophobization, to create the microfluidic channel. Our method involves asymmetric mechanical modification of a paper surface using a rolling ball (ball-point pen) under a controlled amount of applied stress (σ_z) to ascertain that only one side is modified. A lubricating solvent (hexane) aids in the selective deformation. The lubricant also serves as a carrier for a perfluoroalkyl trichlorosilane allowing the channel to be made hydrophobic as it is formed. For brevity and clarity, we abbreviated this method as TACH (Targeted Asymmetric Calendaring and Hydrophobization). We demonstrate that TACH can be used to reliably produce channels of variable widths (size of the ball) and depths (number of passes), without affecting the nonworking surface of the paper. Using tomography, we demonstrate that these channels can vary from 10s to 100s of microns in diameter. The created hydrophobic barrier extends around the channel through wicking to ensure no leakages. We demonstrate, through modeling and fabrication, that flow properties of the resulting channels are analogous to conventional devices and are tunable based on associated dimensionless numbers. *Published by AIP Publishing*. [http://dx.doi.org/10.1063/1.4974013]

I. INTRODUCTION

Microfluidic devices emerged from the need for fast, programmable, and affordable manipulation of small quantities of fluids in high-throughput screening, efficient bio-analysis, and automation, among other applications.[1–4] There are two classes of microfluidic devices, viz, (i) open channel, which requires a pump since the channels that are not filled with any solid components; and (ii) closed channel, which relies on capillary wicking since the channels contain a porous network of solid material and hence do not need a pump. In paper-based devices, the closed channels are filled with paper fibers.[5–7] The closed channels, however, cannot be used with heterogeneous samples (where the heterogeneity defines the desired property) because wicking occurs with concomitant sample segregation/separation (paper chromatography). The open channels, on the other hand, can accommodate complex fluidic samples but often require skilled manpower, involve expensive fabrication methods, are sometimes tedious to fabricate, and cannot be prepared in the field (low-resource settings) on demand. To mitigate costs and improve simplicity of these important open channel devices, better materials and rapid, efficient fabrication methods are desired. Paper is a low-cost, renewable, widely available, and biodegradable material. Therefore, it fits the materials' needs for improved microfluidic devices, but its native wetting properties render it incompatible with most environmental or bio-analytical samples.[5,8–21] A range of methods have been developed to control its wetting properties, such as surface modification through particle deposition, wax printing, and sol-gel techniques, among many others.[8,9,16,22–27]

Paper as a material is asymmetric in its porosity across the thickness, a feature that is a consequence of the preparation methods. The core of a paper is often significantly denser than the surfaces, allowing most of the compressive deformation to be driven by an increase in surface fiber density (decreased surface void volume) to match that of the core—as demonstrated in calendaring (Figure 1(a)). We hypothesized that due to the paper's compressibility and asymmetry in porosity, applying the right amount of compressive stress on one of its faces should lead to asymmetric deformation across the thickness with the working surface being deformed without significantly affecting the opposite surface. When such pressure is targeted/localized, and with the appropriate lubrication to mitigate fiber damage, a channel can be created (Figure 2(a)). We[28,29] and others[5,30–36] have shown that paper can be rendered hydrophobic by treatment with alkyl trichlorosilanes (Figures 1(b) and 1(c); see details in the supplementary material Figure S1).[29] We, therefore, hypothesized that co-deposition of an appropriately functionalized silane during the asymmetric calendaring could lead to a channel with desired wetting properties. To avoid fiber breakage and enhance local compressibility, a suitable non-reactive lubricant (hexane) was used. This lubricant, when locally applied can also act as a carrier solvent for the silane (Figure 1(b)).

II. MATERIALS AND METHODS

A. Materials

Whatman No. 1 (VWR, GE Co., USA) and Gel Blotting (GB003 blotting sheets, 15 × 15 cm, Sigma Aldrich, St. Louis, USA) paper were selected for this study. Trichloro (1H, 1H, 2H, 2H perfluorooctyl) silane (97%) and hexane (ACS reagent grade) were obtained from Sigma Aldrich and used as received. Craft cutter, clear tape (sticker paper), and sketch pen (all from Silhouette®, USA) were obtained from Amazon.com. A Chemyx microfluidics pump (Fusion 720, 50/60 Hz) was used with polyethylene tubing (PE 160, 1.14 mm internal diameter, Becton Dickinson, Sparks, MD, USA) and needles (precision glide syringes 18G × 1½ BD Franklin, NJ, USA) for fluid delivery. Polydimethylsiloxane (PDMS) (Sylgard 184 Silicone Elastomer kit, Dow Corning, Inc.) support slabs were secured with Krazy Glue® (Hobby Lobby, Ames, IA) to the channel inlets.

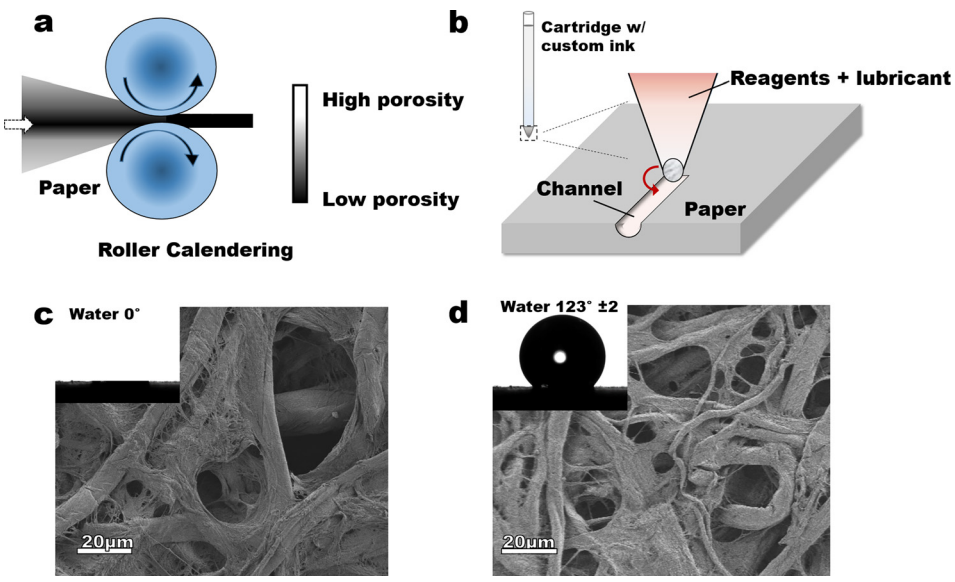

FIG. 1. Schematic of (a) calendaring by roller pressing, and (b) hypothesized calendaring by pressing with a ball point pen. Images of untreated (c) and treated (d) Whatman chromatography no. 1 paper shows no significant changes in the surface structure but significant differences in wetting (inserts capture wetting with water, untreated wicks the droplet of water).

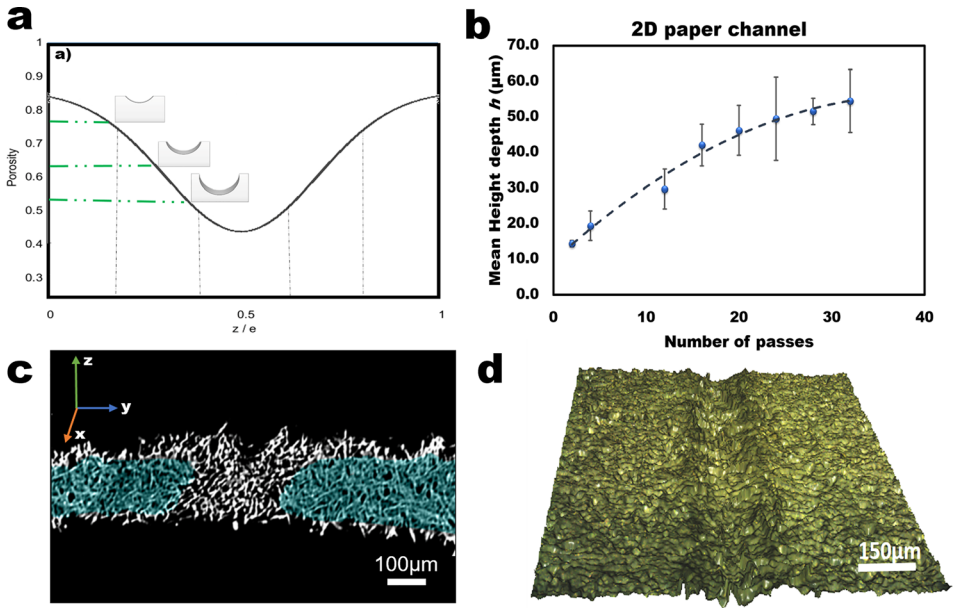

FIG. 2. Summary of results: (a) Expected results from TACH microfluidic channels based on the porosity versus thickness ratio. (b) Quantitative curve of the mean depth profile vs number of passes after calendaring paper by TACH. (c) Capillary movement of water collected by x-ray image of a cross-section of a shallow channel on Whatman no. 1 chromatography paper. (d) Tomography imaging of a deep channel prepared by TACH.

B. Methods

First, a Silhouette® sketching pen was disassembled, the ink cartridge washed with copious amounts of acetone and then air-dried for at least 30 min. The paper was pre-cut into 8×10 cm pieces while the custom ink was prepared by mixing 10 ml of hexane and 1 ml of the fluorinated silane. The custom ink solution (100 μl) was transferred into a clean ink cartridge, the sketch pen reassembled and placed in the holder on the silhouette cutter. The pre-cut paper pieces were placed on the sticky mat of the cutter aligned according to the dimensions of the designed channels as entered on the user interface. The silhouette cutter was set into sketching mode at a speed of 20 cm/min. The resolution of the channel was controlled by the tip diameter, (here ~0.5 mm), while the depth was controlled by the number of passes (repeated sketches). Three designs—"Y," "ㄱ," and "ㄩ"—were drawn on the pre-cut papers. The sticky mat, with the pre-cut paper, was fed into the cutter, and the sketching process was started. The sketching was repeated ten times (number of passes) to create deeper channels without passing through the entire thickness of the paper. After sketching, the paper samples were removed from the mat and placed in the fume hood for 20 min to allow the hexane to evaporate from the surface of the paper. Alternatively, the process was expedited by placing the channels in a desiccator and applying vacuum. The channels were characterized using contactless profilometry and X-ray tomography (ESRF beamline ID 19, Grenoble, France). To fabricate a working device, the channels were covered with transparent tape on which either two inlets and/or an outlet had been pre-cut. The inlets could also be created by punching small holes on the channel inlets and attaching the tubing from the back of the device (Figure 3(a)).

III. RESULTS AND DISCUSSION

The reaction of the appropriate alkylsilane, from either gas or liquid phase, with hydroxylated surfaces like paper gives hydrophobic surface. In these chemical grafting reactions, it is often assumed that self-assembled monolayers form on the surface. We recently demonstrated[29] that the reaction of a perfluoro trichlorosilane with cellulose, albeit via solid-vapor reaction,

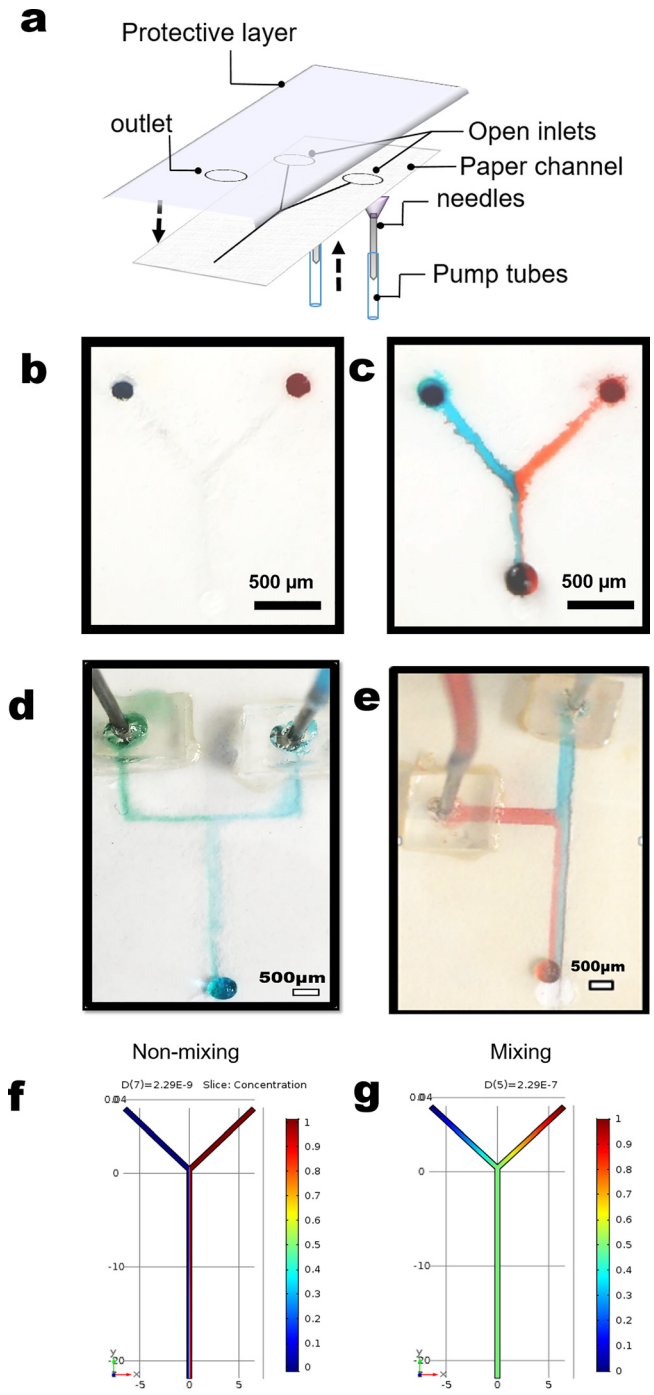

FIG. 3. Paper-based open-channel microfluidic devices derived from TACH. (a) Schematic assembly of a device. A fabricated device before (b) and after (c) introducing liquid in the channel at 0.1 mil/min flow rate. (d) and (e) Top inlet designs of TACH performed showing laminar flow on different designs and dimensions. (f) and (g) Concentration evolution along the length of a cross-section of the channel from the inlet (top) to the outlet (bottom). Almost non-mixing (left for Pe = 8.6 $\times$ 10^6) or mixing (right for Pe = 0.86) operating conditions can either be selected, validating the possibility to use paper for microfluidics devices.

occurs via a step-growth polymerization mechanism and leads to ultra-hydrophobic (water static contact angle, $\theta s > 120°$) surfaces. This reaction (supplementary material, Figure S1) involves recruitment of surface bound water to pre-oligomerize the silane prior to surface attachment. Silanization of Whatman chromatography paper no. 1 creates ultra-hydrophobic (defined by

contact angles between 121° and 149°)[29] surfaces ($\theta s = 123° \pm 2$) as shown above (Figures 1(c) and 1(d)).

A. Surface characterization

Channels were created without perturbing the porosity and fiber structure of the nonworking surface (Figure 2(c) and supplementary material Figure S3). Assuming asymmetric calendaring-type deformation, the channel depth was expected to increase with the number of sketching passes (Figure 2(a)) and was found to be tunable based on the calibration curve (Figure 2(b)). The depth profile and fiber organization were mapped using a surface profilometer in contactless mode (Figure 2(d)). From the analysis of the fiber structure on the unstressed (non-calendared) regions, we can ascertain that the fiber organization does not change but the porosity of the paper changes with the number of passes (voids are decreased). These results suggest that our process is analogous to calendaring and not embossing, where fiber damage is rampant. To ascertain and demonstrate the extent of the chemical treatment, prepared channels were dried *in vacuo* (~30 mmHg) at 70 °C, and then shipped by courier from the United States to France for synchrotron-based x-ray tomography. We observed that the prepared samples were still hydrophobic and water did not wick around the channels (Figure 3(c)). To ascertain the resilience of the treatment, a comprehensive study is underway and will be reported in an appropriate platform.

In Figure 2(c), wicking (wetted) regions are false-colored for clarity (samples of non-colorized images are given in the supplementary material Figure S3). We observe that, as expected, the hydrophobic region is radially oriented around the channel and correlates with the number of passes. This result indicates that the more passes we make, the deeper the channel and the wider the silane reagent spreads. We observe that whether we fabricated narrow or wide channels, the extent of the hydrophobic barrier correlates with the number of passes and is not dependent on the channel shape (supplementary material Figure S3). A calibration curve for use in controlling channel depth by changing the number of passes was developed using straight single line channels (Figure 2(b)). To ascertain that fiber organization does not change, all three channel designs were characterized using surface profilometry to ascertain that corners were not different from the rest of the channels. To further ascertain that the chemical modification does not degrade over time, we are monitoring a structure over extended periods of time (target 24 months) and so far (ca. 6 months) we have not observed any significant changes in the hydrophobicity. A comprehensive report of the resilience of this coating is the subject of an upcoming report.

B. Channel fabrication

The resulting channels had width dimensions of up to ~250 μm. To validate the capability of fabricated channels as microfluidic devices, a "Y" design was used for fluid flow and theoretically compared with the literature (Figures 3(a)–3(c)).[5,8,10,11,14,16,18,20,37–43] Other geometries were also fabricated (Figures 3(d) and 3(e)) to show the versatility of the targeted asymmetric calendaring and hydrophobization (TACH) method. The microfluidic devices were manufactured using paper and tested with dyed water (food color) for visualization. Once the channels had been created, they were covered with tape and inlets, consisting of a needle, and the PE tubing was attached as shown in Figure 3(a) (see also supplementary material Figures S4 and S5). Extra care was taken during the fabrication of the devices to avoid collapsing of these rather small delicate channels. Inlets were attached using PDMS supports and double-sided tape. The channels were then infused with water (containing food color for clarity) at different flow rates based on channel dimensions and as predicted from simulations (see discussion below and in the supplementary material). The fabrication from channel design to a working device can be completed within 20 min. Three types of designs were fabricated (Figures 3(b)–3(e)). Due to the low flow rate, the T-device showed laminar flow as opposed to droplet generation. We exercised caution in the range of flow rates that we could test to avoid over-pressurizing

the channels, which could lead to delamination or leakage through the porous structure of the paper.

Since paper is a porous material, this can be viewed as one of the weaknesses of these devices, although others have exploited this porosity to diversify the dimensions of the resulting channels.[5] Since TACH does not lead to deformation of the overall paper surface, we evaluated the versatility of stacking as a tool to tune the channel depth (supplementary material Figures S4c and S4d). We demonstrated that one can easily exploit the stack ability of paper to tune (adjust) the depth of created channels (Figure 3(e)). We exploit the stackability of paper, as previously shown[5,9] to demonstrate that when multiple papers are stacked, the depth, and hence flow properties, of the channels can be tuned. This property has been widely used in microfluidic devices and we demonstrate that it is not lost with TACH.

C. Theoretical understanding of fabricated channels

In microfluidics, dimensionless numbers such as the Reynolds or the Péclet numbers are widely used to evaluate the importance of each of the numerous competing phenomena occurring in the liquid. For instance, mixing is typically enhanced at high Reynolds numbers (>1000, turbulent flows) by the movement of the eddies, but it is not uncommon in microfluidics to observe mixing through diffusion (Péclet number < 1) at low Reynolds number (<1000, laminar or Stokes flows). In ┐ or Y channel geometries, mixing is typically desired, for example, in sensing[44] or filtering[45] purposes, while non-mixing flows can be used to fabricate microstructures within pre-existing channels[46] or for the study of biological systems.[47] Here, we used numerical simulations to evaluate versatility of paper microfluidic devices fabricated through the TACH approach. The impact of the governing parameters (e.g., velocity of the flow or diffusion coefficient of the liquid) required to trigger (or inhibit) mixing and/or obtain the desired flow characteristics will also be evaluated. Assuming the liquid is (or near) stationary, the governing equations are as follows: Navier Stokes

$$\rho \nabla u = 0; \quad \rho(u\nabla)u = -\nabla p + \mu\nabla[(\nabla u + {}^{t}\nabla u)],$$

and convection-diffusion

$$u.\nabla c_\alpha = D_\alpha \nabla^2 c_\alpha,$$

where u is the velocity field, ρ is the pressure, c_α is the concentration of the solute α, and D_α is the diffusion coefficient. By writing these equations in a dimensionless form, Reynolds and Péclet numbers are revealed from the Navier-Stokes and convection-diffusion equation, respectively, with

$$R_e = \frac{\rho L U}{\mu} \quad \text{and} \quad P_e = \frac{UL}{D},$$

in which L and U are the characteristic length and velocity, respectively. Note that L has been chosen here as the width (w) of the channel to estimate the Reynolds number and as the length (l) of the channel to estimate the Péclet number, as commonly observed in microfluidics. Typically, a flow for which the $R_e < 1000$ will be laminar, and if the $P_e < 1$, mixing will occur by diffusion.

The stationary governing equations were solved for a 3D geometry in COMSOL Multiphysics®. The geometry simulated was based on the experimental Y device, with equivalent dimensions to that shown in Figure 3(b). The Reynolds number was varied in the range $0.5 \times 10^{-3} < \mathrm{Re} < 500$, by changing the inlet flow rate from $\mathrm{Q} = 10^{-4}$ ml/min to $\mathrm{Q} = 1$ ml/min and keeping the physical properties of the channels and fluid constant (i.e., $\mathrm{w} = 50\,\mu$m, $\mathrm{l} = 30$ mm, $\rho = 1000$ kg/m^3, and $\mu = 1$ mPa s). The Péclet number was varied from $10^{-4} < \mathrm{Pe} < 10^{10}$ by changing the flow rate and the diffusion coefficient from $\mathrm{D} = 2.29 \times 10^{-4}$ m^2/s to $\mathrm{D} = 2.29 \times 10^{-9}$ m^2/s and keeping the length of the channel constant. The values of the diffusion coefficient have been selected in that range because $\mathrm{D} = 2.29 \times 10^{-9}$ m^2/s is the self-diffusion

coefficient of water and $D = 10^{-4}$ m^2/s is the self-diffusion coefficient of H_2.[48] For simulation purposes, the concentration of one of the inlets has been fixed to 0 and the other inlet to 1. As shown in Figures 3(f) and 3(g), the devices fabricated here can either be used to mix liquids or maintain laminar flows depending on the value of the Péclet number (S6–S10). It is shown that a triangular configuration helps to reduce the friction losses for a constant cross-section area, as expected by theoretical considerations (S8). From here, we can, therefore, infer that using TACH, flow behavior can be tuned as needed to either maintain laminar or stokes flow or induce significant mixing through channel size and shape. The shape of the channel can be varied based on the rolling ball of the ball-point pen (see supplementary material, Figure S3(a) vs S3(b)).

IV. CONCLUSION

We have developed a method to fabricate open-channel microfluidic devices by selectively calendaring one surface of a single sheet of paper without significantly affecting the opposite surface. By coupling the mechanical stress with chemical modification, we created hydrophobic channels on a porous surface allowing the flow of mixed liquids akin to conventional microfluidic devices. By exploiting the stack-ability of paper, channel dimensions can be tuned to accommodate the desired flow profiles. We achieved this without significant damage to the fibers, since calendaring does not lead to fiber reorganization but instead reduces porosity. We demonstrate, through numerical simulations, that the obtained channels are comparable to conventional microfluidics, albeit at a significantly lower cost and ease of fabrication. The cost of each device (assuming 3 μl per device) is estimated to be ~\$0.003 under laboratory settings. The overall production can also be automated and requires unskilled manpower making TACH a potentially rapid, efficient, and cost-effective approach to manufacturing lab-on-chip and other related technologies. Where access to technology is not a problem, this method can be improved by using a relief printing process with concomitant deposition of the reactive ink (to create hydrophobic barriers) with the caveat that the reliefs must be targeted and use low pressure to avoid modification of both sides of the paper akin to embossing.

SUPPLEMENTARY MATERIAL

See supplementary material for details on the simulation ran for the channels, a discussion on mixing, as well as non-colorized tomography images and schematic overview of other paper-based microfluidic device fabrication techniques.

ACKNOWLEDGMENTS

This research was supported by start-up funding from Iowa State University and a Black and Veatch faculty fellowship to M.T. S.O.-R. was supported by GMAP fellowship. J.C. was supported through a Catron fellowship from Catron Solar Energy Center. Support from the European Synchrotron Radiation Facility (ESRF), Grenoble, is acknowledged. This work was carried in part at the Center for Nanoscale Systems (CNS), a member of the National Nanotechnology Infrastructure Network (NNIN), which was supported by the National Science Foundation under NSF Award No. ECS-0335765. CNS is part of Harvard University. We thank Rafael Luna of Luna Scientific Storytelling.

[1]A. Persidis, Nat. Biotechnol. **16**(5), 488 (1998).
[2]J.-H. Zhang, T. D. Y. Chung, and K. R. Oldenburg, J. Biomol. Screening **4**(2), 67–73 (1999).
[3]T. Colbert, B. J. Till, R. Tompa, S. Reynolds, M. N. Steine, A. T. Yeung, C. M. McCallum, L. Comai, and S. Henikoff, Plant Physiol. **126**(2), 480–484 (2001).
[4]K. H. Bleicher, H.-J. Böhm, K. Müller, and A. I. Alanine, Nat. Rev. Drug Discovery **2**(5), 369–378 (2003).
[5]M. M. Thuo, R. V. Martinez, W.-J. Lan, X. Liu, J. Barber, M. B. J. Atkinson, D. Bandarage, J.-F. Bloch, and G. M. Whitesides, Chem. Mater. **26**(14), 4230–4237 (2014).
[6]N. Herzer, S. Hoeppener, and U. S. Schubert, Chem. Commun. **46**(31), 5634–5652 (2010).
[7]S.-W. Lee, J.-Y. Noh, S. C. Park, J.-H. Chung, B. Lee, and S.-D. Lee, Langmuir **28**(20), 7585–7590 (2012).
[8]Y. Lu, W. Shi, L. Jiang, J. Qin, and B. Lin, Electrophoresis **30**(9), 1497–1500 (2009).
[9]E. Carrilho, A. W. Martinez, and G. M. Whitesides, Anal. Chem. **81**(16), 7091–7095 (2009).

[10]W. Dungchai, O. Chailapakul, and C. S. Henry, Analyst **136**(1), 77–82 (2011).
[11]X. Li, D. R. Ballerini, and W. Shen, Biomicrofluidics **6**(1), 011301 (2012).
[12]B. Gao, H. Liu, and Z. Gu, Anal. Chem. **88**(10), 5424–5429 (2016).
[13]A. W. Martinez, S. T. Phillips, B. J. Wiley, M. Gupta, and G. M. Whitesides, Lab Chip **8**(12), 2146–2150 (2008).
[14]A. W. Martinez, S. T. Phillips, G. M. Whitesides, and E. Carrilho, Anal. Chem. **82**(1), 3–10 (2010).
[15]W. K. T. Coltro, D. P. de Jesus, J. A. F. da Silva, C. L. do Lago, and E. Carrilho, Electrophoresis **31**(15), 2487–2498 (2010).
[16]G. Chitnis, Z. Ding, C.-L. Chang, A. Savran Cagri, and B. Ziaie, Lab Chip **11**(6), 1161–1165 (2011).
[17]L. Ge, S. Wang, X. Song, S. Ge, and J. Yu, Lab Chip **12**(17), 3150–3158 (2012).
[18]J. Nie, Y. Zhang, L. Lin, C. Zhou, S. Li, L. Zhang, and J. Li, Anal. Chem. **84**(15), 6331–6335 (2012).
[19]N. R. Pollock, J. P. Rolland, S. Kumar, P. D. Beattie, S. Jain, F. Noubary, V. L. Wong, R. A. Pohlmann, U. S. Ryan, and G. M. Whitesides, Sci. Transl. Med. **4**(152), 152ra129 (2012).
[20]P.-K. Kao and C.-C. Hsu, Anal. Chem. **86**(17), 8757–8762 (2014).
[21]E. K. Sackmann, A. L. Fulton, and D. J. Beebe, Nature **507**(7491), 181–189 (2014).
[22]J. C. Pouxviel and J. P. Boilot, J. Non-Cryst. Solids **94**(3), 374–386 (1987).
[23]W. G. Klemperer and S. D. Ramamurthi, J. Non-Cryst. Solids **121**(1), 16–20 (1990).
[24]K. A. Mauritz, Mater. Sci. Eng., C **6**(2–3), 121–133 (1998).
[25]N. Kiraz, E. Burunkaya, O. Kesmez, M. Asilturk, H. E. Camurlu, and E. Arpac, J. Sol-Gel Sci. Technol. **56**(2), 157–166 (2010).
[26]T. Textor and B. Mahltig, Appl. Surf. Sci. **256**(6), 1668–1674 (2010).
[27]J. Yadav, M. Datta, and V. S. Gour, BioResources **9**(3), 5066–5072, 5067 (2014).
[28]S. Oyola-Reynoso, I. Tevis, J. Chen, B. S. Chang, S. Cinar, J.-F. Bloch, and M. M. Thuo, J. Mater. Chem. A. **4**, 14729–14738 (2016).
[29]S. Oyola-Reynoso, I. Tevis, J. Chen, J. F. Bloch, and M. Thuo, Procedia Eng. **141**, 59–62 (2016).
[30]B. Chen, P. Kwong, and M. Gupta, Appl. Mater. Interfaces **5**(23), 12701–12707 (2013).
[31]P. Samyn, Mater. Sci. **48**(19), 6455–6498 (2013).
[32]A. C. Glavan, D. C. Christodouleas, B. Mosadegh, D. Yu Hai, B. S. Smith, J. Lessing, T. M. Fernandez-Abedul, and G. M. Whitesides, Anal. Chem. **86**(24), 11999–12007 (2014).
[33]A. C. Glavan, R. V. Martinez, A. B. Subramaniam, H. J. Yoon, R. M. D. Nunes, H. Lange, M. M. Thuo, and G. M. Whitesides, Adv. Funct. Mater. **24**(1), 60–70 (2014).
[34]S. Oyola-Reynoso, A. P. Heim, J. Halbertsma-Black, C. Zhao, I. D. Tevis, S. Çınar, R. Cademartiri, X. Liu, J.-F. Bloch, and M. M. Thuo, Talanta **144**, 289–293 (2015).
[35]Z. Tang, H. Li, D. W. Hess, and V. Breedveld, Cellulose **23**(2), 1401–1413 (2016).
[36]D. E. Damon, K. M. Davis, C. R. Moreira, P. Capone, R. Cruttenden, and A. K. Badu-Tawiah, Anal. Chem. **88**(3), 1878–1884 (2016).
[37]D. A. Bruzewicz, M. Reches, and G. M. Whitesides, Anal. Chem. **80**(9), 3387–3392 (2008).
[38]A. Bhattacharyya and C. M. Klapperich, Anal. Chem. **78**(3), 788–792 (2006).
[39]F. B. Myers and L. P. Lee, Lab Chip **8**(12), 2015–2031 (2008).
[40]X. Mao and T. J. Huang, Lab Chip **12**(8), 1412–1416 (2012).
[41]A. Nilghaz, D. H. B. Wicaksono, D. Gustiono, F. A. A. Majid, E. Supriyanto, and M. R. A. Kadir, Lab Chip **12**(1), 209–218 (2012).
[42]W. K. Tomazelli Coltro, C. M. Cheng, E. Carrilho, and D. P. Jesus, Electrophoresis **35**(16), 2309–2324 (2014).
[43]B. M. Jayawardane, I. D. McKelvie, and S. D. Kolev, Anal. Chem. **87**(9), 4621–4626 (2015).
[44]C. N. Baroud, F. Okkels, L. Ménétrier, and P. Tabeling, Phys. Rev. E **67**(6), 060104 (2003).
[45]B. S. Cho, T. G. Schuster, X. Zhu, D. Chang, G. D. Smith, and S. Takayama, Anal. Chem. **75**(7), 1671–1675 (2003).
[46]P. J. A. Kenis, R. F. Ismagilov, and G. M. Whitesides, Science **285**(5424), 83–85 (1999).
[47]A. Sawano, S. Takayama, M. Matsuda, and A. Miyawaki, Dev. Cell **3**(2), 245–257 (2002).
[48]M. Holz, S. R. Heil, and A. Sacco, Phys. Chem. **2**(20), 4740–4742 (2000).